AGU PUBLICATIONS

JGR

Journal of Geophysical Research: Solid Earth

RESEARCH ARTICLE
10.1002/2017JB014291

Key Points:
- Data are from 18 seismic stations in Libya
- Receiver functions (RFs) are used to infer crustal thickness (H) and ratios of V_p/V_s (κ)
- Crustal thickness in Libya ranges from 24 to 36 km
- A high V_p/V_s (κ) ratio of 1.91 at the AS Sawda Volcanic Province indicates the presence of melt
- The crust in this region would seem to be older than the Phanerozoic

Supporting Information:
- Supporting Information S1
- Figures S1–S12
- Data Set S1
- Data Set S2

Correspondence to:
A. A. Lemnifi,
aalmwb@mst.edu

Citation:
Lemnifi, A. A., Elshaafi, A., Browning, J., Aouad, N. S., El Ebaidi, S. K., Liu, K. K., & Gudmundsson, A. (2017). Crustal thickness beneath Libya and the origin of partial melt beneath AS Sawda Volcanic Province from receiver function constraints. *Journal of Geophysical Research: Solid Earth*, *122*, 10,037–10,051. https://doi.org/10.1002/2017JB014291

Received 6 APR 2017
Accepted 13 OCT 2017
Accepted article online 21 OCT 2017
Published online 7 DEC 2017

Crustal Thickness Beneath Libya and the Origin of Partial Melt Beneath AS Sawda Volcanic Province From Receiver Function Constraints

Awad A. Lemnifi[1,2], Abdelsalam Elshaafi[2,3], John Browning[4], Nassib S. Aouad[1], Saad K. El Ebaidi[2], Kelly K. Liu[5], and Agust Gudmundsson[3]

[1]Mining Engineering Department, Missouri University of Science and Technology, Rolla, MO, USA, [2]Department of Earth Sciences, Faculty of Sciences, Benghazi University, Benghazi, Libya, [3]Department of Earth Sciences, Royal Holloway, University of London, Egham, UK, [4]Department of Earth Sciences, University College London, London, UK, [5]Geology and Geophysics Program Missouri University of Science and Technology, Rolla, MO, USA

Abstract This study investigates crustal thickness and properties within the Libyan region. Results obtained from 15 seismic stations belonging to the Libyan Center for Remote Sensing and Space Science are reported, in addition to 3 seismic stations publically available, using receiver functions. The results show crustal thicknesses ranging from 24 km to 36 km (with uncertainties ranging between ±0.10 km and ±0.90 km). More specifically, crustal thickness ranges from 32 km to 36 km in the southern portion of the Libyan territory then becomes thinner, between 24 km and 30 km, in the coastal areas of Libya and thinnest, between 24 km and 28 km, in the Sirt Basin. The observed high V_p/V_s value of 1.91 at one station located at the AS Sawda Volcanic Province in central Libya indicates the presence of either partial melt or an abnormally warm area. This finding suggests that magma reservoirs beneath the Libyan territory may still be partially molten and active, thereby posing significant earthquake and volcanic risks. The hypothesis of an active magma source is further demonstrated though the presence of asthenospheric upwelling and extension of the Sirt Basin. This study provides a new calculation of unconsolidated sediment layers by using the arrival time of the *P* to *S* converted phases. The results show sediments thicknesses of 0.4 km to 3.7 km, with the V_p/V_s values ranging from 2.2 to 4.8. The variations in crustal thickness throughout the region are correlated with surface elevation and Bouguer gravity anomalies, which suggest that they are isostatically compensated.

1. Introduction

1.1. Tectonic Setting and Origin of Volcanism

In the last decades, many studies have suggested that the current continental crust reflects multiple accretionary processes resulting from continent-continent collision, volcanic arcs, continental rifting, and basaltic volcanism at hot spots (Christensen & Mooney, 1995; Clarke & Silver, 1993; Griffin & O'Reilly, 1987; Lemnifi et al., 2017; Rudnick & Fountain, 1995; Rudnick & Gao, 2003). Most of the African subcontinental lithospheric mantle (SCLM) is believed to be of Archean origin but strongly affected by metasomatization during later geological events (Begg et al., 2009). The subcontinental lithosphere is composed of cratons and smaller cratonic fragments that are linked together by younger fold belts. The boundaries of these fragments are fed by magmas that over time generate a fertilization of the SCLM. These weak margins undergo many cycles of rifting, extension, subduction, and renewed accretion (Begg et al., 2009).

The North African portion of the subcontinental lithospheric mantle has undergone a series of complex tectonic processes, where the most notable being the Pan-African events. The Pan-African events (Late Proterozoic to Early Paleozoic) developed continental-scale convergence structures, such as crustal thickening, and may be related to volcanic arcs and possibly deeper alterations indicated by drop a Bouguer gravity anomaly (Doucouré & de Wit, 2003; Liégeois et al., 2013, 2005; Liu & Gao, 2010; Van Der Meijde et al., 2003). Libya includes a portion of the largest Archean craton of Africa, which is the Sahara Metacraton (SMC). The SMC extends from the Tuareg Shield to the Arabian-Nubian Shield (Abdelsalam et al., 2002; Lemnifi et al., 2015). According to geochronological and isotopic data, the whole craton appears to have behaved as a single block during the Phanerozoic (Abdelsalam et al., 2002; Liégeois et al., 2013). In addition, the Late

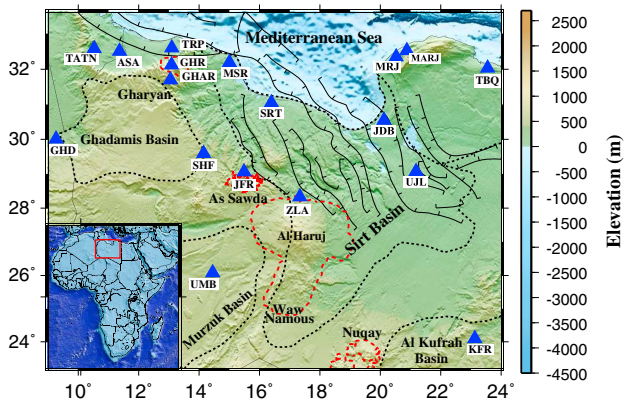

Figure 1. Map illustrating the topography of the study area with the locations of seismic stations used in this study, which are indicated by blue triangles. The boundaries of sedimentary basins are represented by black dashed lines (Hassan & Kendall, 2014). The main volcanic provinces and Mesozoic rifts with teeth on downthrown blocks are indicated by red and black dashed lines, receptively (Guiraud & Bosworth, 1997). Inset map shows the location of the study area in Africa.

Paleozoic oceanic crust is found north of the continental crust of Libya and Egypt (Granot, 2016; Speranza et al., 2012).

A series of uplifts have been recognized on the surface of the SMC, such as the western Tihemboka uplift, the Tibesti-Sirt uplift, the Tripoli-Tibesti uplift, the Al Garaqaf arch, the Haruj Uplift, and the eastern Calanscio-Awayant uplift (Craig et al., 2008; Hassan & Kendall, 2014). The Phanerozoic period in the north of Africa involved episodic compressional and extensional tectonism (Nyblade et al., 1996). During the Mesozoic and early Cenozoic, the North African part was affected mainly by subduction of the Mesozoic lithosphere along the Hellenic arc and Calabrian arc (Capitanio et al., 2009; Marone et al., 2003). In the same period, deep-seated rifting and marine transgression across the region was initiated. As a result, many basins were formed, such as the Sirt, the Murzuk, the Al Kufrah, and the Ghadamis Basins as illustrated in Figure 1. In the northern part of central Africa, there is significant continental extension (represented by normal faults) affecting an area of 500 km in width and 500 km in length along the Sirt Basin. This extension developed during the Late Cretaceous to the Eocene, and perhaps into the Holocene, and may have been controlled by the slab pull force developed during the Hellenic convergent event in the north of the region (Capitanio et al., 2009; Nyblade et al., 1996).

Volcanism in Libya began in the Eocene and continued developing into the late Pleistocene. Some evidence suggests volcanism continued along the western and southwestern margins of the Sirt Basin into the Holocene (Elshaafi & Gudmundsson, 2016, 2017a; Nixon et al., 2011). Volcanic units of the Al-Haruj province of Libya are dominated by primarily olivine- and clinopyroxene-rich magma types, which were likely sourced from the juvenile asthenosphere (Cvetković et al., 2010). It has been proposed that the extrusion of these volcanic units occurred during the reactivation of older lithospheric faults from the uplift events (Cvetković et al., 2010). Basaltic rocks of Libya's volcanism were produced by melting of predominately anhydrous mixed peridotitic mantle source in an upper mantle plume with an asthenosphic potential temperature around 1400°C (Ball et al., 2016; Nixon et al., 2011).

The origin of magma beneath Libya and North Africa at large scale is still poorly understood and widely debated. For example, Hegazy (1999) argues that the Libyan intraplate volcanism is related to hot mantle plumes in the underlying asthenosphere. Keppie et al. (2011) propose a conceptual model, using available geophysical and geological constraints, outlining the geometry of a channel plume underlying North Africa, which laterally feeds geographically discrete volcanic fields, similar to a model of the Afar plume (cf. Ebinger & Sleep, 1998). Tomographic models by Begg et al. (2009) argue that topography of the bottom of cratonic blocks in Africa has caused an important role in guiding the upwelling hot mantle, whereby magma might ascend to the surface through metasomatized lithospheric channels. Based on geochemistry and isotope data, Nixon et al. (2011) infer that the North African Tertiary-Quaternary volcanism can be partly explained in terms of diapiric upwellings originating from the upper mantle.

The main volcanic provinces in Libya mostly coincide with the current elevated basement regions. There are at least two alternative mechanisms that may explain this relationship between basement and volcanic provinces in Libya: (i) the regions have been subject to magmatic underplating that led to further increase in the elevation (cf. Craig et al., 2011) and (ii) the basement highs have been subject to subcrustal arching (Al-Hafdh & El-Shaafi, 2015; Vail, 1971).

All these studies and related models to a large degree depend on having a reasonably accurate knowledge of the crustal thickness beneath Libya. However, the crustal thickness of Libya and of the central North Africa, in general, has been rather poorly constrained, partly because of the paucity of seismic broadband stations. The results of receiver function (RF) investigations on the crustal thickness of Libya are presented in this study. In particular, the aim of this paper is to present new results on the total thickness of the crust (H) beneath the seismic stations, as well as the bulk P to S wave velocity ratio (V_p/V_s, hereafter denoted κ; cf. Christensen, 1996). The crustal thickness results are discussed in relation to models on the distribution of partial melt (magma accumulation) and proposed mantle plumes beneath parts of Libya, as well as the resulting extensive volcanism.

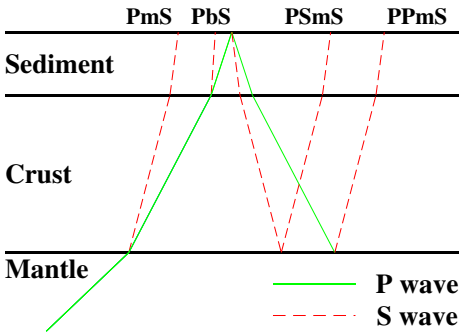

Figure 2. Simplified cross section showing the main P_s converted phases (*PmS*, *PbS*, *PSmS*, and *PPmS*) at the crust-mantle and sediment-crust boundaries.

This research pioneers the efforts in studying the crustal thickness beneath Libya. A major problem for the seismicity studies of Libya in past decades was the absence of any extensive seismological network until 2005 at which time the first Libyan seismological network was established (Al-Heety, 2013). Specifically, this study uses seismologic data acquired from 2005 to 2009 and allows us to infer in much greater detail than has been possible before the depth of Moho in various parts in Libya and, in particular, the origin of the partial melting within the AS Sawda Volcanic Province, central Libya. The results of a detailed analysis of stacked RFs from all available new seismic stations are reported by examining all associated *P* to *S* converted phases (P_mS, PP_mS, and PS_mS, hereafter collectively known as P_xS) (Figure 2) throughout Libya.

1.2. Previous Geophysical Studies

Many geophysical studies have focused on crustal thicknesses beneath northern and central Africa (Begg et al., 2009; Marone et al., 2003; Pasyanos & Nyblade, 2007; Pasyanos & Walter, 2002) using different global velocity models. Marone et al. (2003) estimated the crustal thickness at the Eurasia-Africa plate boundary on basis of receiver function analysis, reflection and refraction surveys, and gravity and anomaly measurements. They inferred a typical Moho depth of about 30 km. They interpreted the sharp change in crustal thickness along the coast of Africa (from 25 km to 35 km) as being due to extension of the North African margin. In this area Moho depth and structure are poorly constrained, making it difficult to provide reliable models of associated local geological processes.

Sandvol et al. (1998) used H-κ stacking to estimate the crustal structure in the Middle East and in a segment of North Africa but did not include data from Libya. Van Der Meijde et al. (2003) studied the crustal structure beneath the Mediterranean region using H-κ stacking and found that the crustal thickness varies from 22 km beneath the intraoceanic islands to 47 km beneath the continental margins. They found a deeper Moho of 30 ± 2.1 km at station GHAR and 31 ± 1.5 km at station MARJ (Figure 1). In their study, they chose the peaks by using a very broad grid search method, so the Moho depth could range from 30 km to 36 km for both stations in their study. Pasyanos and Nyblade (2007) estimated crustal thickness beneath Africa and Arabia using forward modeling of surface waves and found that the crustal thickness in the study area varies between 25 km and 35 km. They found that the crustal thickness at the coastline is about 25 km in the west and 30 km to 35 km in the east. They also have examined the sedimentary cover thickness in the African and Arabian platforms, including that in the study area, providing estimates indicating that the sediment layers are thicker in the coastal areas (about 3.5 km to 5.5 km) and thinner in the central portions (about 1.0 km to 3.0 km).

The gravity field of the eastern Mediterranean Sea, including the coastline of the study area, was studied by Cowie and Kusznir (2012) whose results indicate that close to the coastline the offshore crust is about 35 km thick but 20–25 km thick farther seaward, while in the interior of Libya the crust reaches its maximum thickness of 40–45 km. They concluded that the thickness of sedimentary deposits along the southern coastline of the Mediterranean Sea is ranging from 4 km to 6 km.

High heat flow of 80–120 mW/m^2 in northwestern Africa is associated with a regional thermal anomaly in the lithosphere (Lesquer et al., 1990). Specifically, the Tertiary-late Quaternary volcanic activity in Algeria, in the Hoggar massif, indicates that the upper mantle beneath northwestern Africa is still partially molten (Lesquer et al., 1990; Nyblade et al., 1996). Very low shear wave velocities (V_s) have been observed beneath eastern Africa and branches throughout northern Africa, which may reflect the presence of partial melt at the crust-mantle boundary (Begg et al., 2009; Deen et al., 2006).

2. Data and Methods

We used receiver functions (RFs) obtained from 15 seismic stations managed by the Libyan Center for Remote Sensing and Space Science (LCRSSS) and 3 seismic stations from the Incorporated Research Institutions for Seismology (IRIS) and Data Management Center (DMC). The operation period of the Libyan Network stations ranged from early 2005 to late 2009, while the data were acquired from early 2000 to 2013 for the public seismic stations. All 18 stations were used to estimate H and κ values, using the method of Zhu and Kanamori (2000). Figure 3 shows the distribution of earthquakes used in this study from both seismic networks.

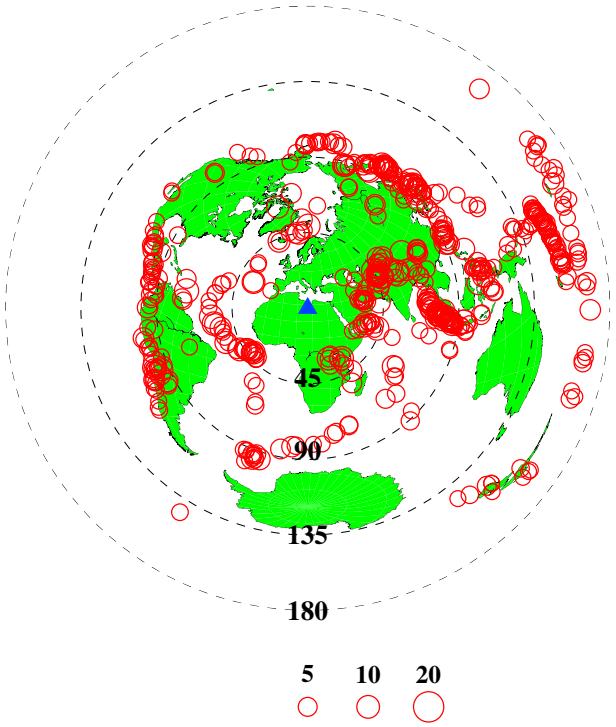

Figure 3. Location of the events used in this study. The size of the red circles is proportional to the number of high-quality receiver functions from that event. The blue triangle indicates the area of study.

The three component seismograms are adjusted to 20 s earlier and 260 s after the first *P* wave arrival based on the IASP91 Earth model, and seismograms were filtered in the 0.04–0.8 Hz frequency band to enhance the signal-to-noise ratio. All seismic events in this study have magnitudes between 5.2 and 6.2 and occurred at epicentral distances from 30° to 180° (cf. Liu et al., 2017; Nair et al., 2006; Reed et al., 2014) (Figure 3). In this study, the cutoff magnitude (M_c) was defined as $M_c = 5.2 + (D_e - 30.0)/(180.0-30.0) - H_f/700$, where D_e is epicentral distance in degree and H_f is focal depth in kilometer (Liu & Gao, 2010). We applied the procedure of Ammon (1991) to deconvolving the vertical component from the radial component to filter seismograms with a *P* wave signal. A signal-to-noise ratio of 4.0 or greater was used in order to generate radial RFs on the radial component utilizing the frequency domain water level deconvolution. This method uses the relative arrival times of the *P* wave and associated *P* to *S* converted phases P_xS by grid searching each station's stacked trace across a range of candidate values for *H* and κ. A constant *P* wave crustal velocity of 6.5 km/s was assumed in this study. The optimal pair of *H* and κ values was investigated in the range of 15–55 km and 1.65–1.95, with the intervals of 0.1 km and 0.01 km, respectively.

Moreover, the high-quality seismograms were manually selected with a robust first arrival of the direct *P* phase on the vertical component in order to identify the optimal pair of *H* and κ corresponding to the maximum stacking amplitude (Zhu & Kanamori, 2000). Thus, iterating the moveout corrections and stacking were used to determine the parameters (*H* and κ) and their standard deviations (uncertainties) through 10 bootstrap computation using the Efron and Tibshirani (1986) method for random resampling in order to obtain a reliable estimate. We used a producer that is described by Zhu and Kanamori (2000) to stack the RFs. The following equation describes the stacking of the receiver functions at each of the station.

$$A(H_i, \kappa_j) = \sum_{k=1}^{N} w_1 \times S_k\left(t_1^{(i,j)}\right) + w_2 \times S_k\left(t_2^{(i,j)}\right) - w_3 \times S_k\left(t_3^{(i,j)}\right), \quad (1)$$

where *N* is the number of high-quality radial RFs from the station, $S_k(t)$ is the amplitude of the point on receiver function at time *t* after the direct *P* arrival, t_1, t_2, t_3 are the moveout times for the P_xS, and the w_1, w_2, and w_3 are the weighting that satisfy $w_1 + w_2 + w_3 = 1$ (Zhu & Kanamori, 2000). More detailed descriptions of this method can be found in Nair et al. (2006) and in Reed et al. (2014). The stations results were ranked as follows: A (*excellent*), B (*good*), and C (*poor*) according to the peak clarity of the P_xS on the *H*-κ. Those stations assigned a rank of C were not included in the results.

The study area has four major sedimentary basins as already mentioned, and stations SRT, MSR, UJL, ZLA, SHF, UMB , GHD, and KFR are located within the sedimentary basins (Figure 1). The Mesozoic Sirt Basin situated in north central Libya is bounded by the Paleozoic Ghadamis, Murzuk, and Al Kufrah Basins. These basins have thick sedimentary deposits, ranging from 1 km to 7 km (Abadi et al., 2008; Hassan & Kendall, 2014; Pasyanos & Nyblade, 2007). The increasing thickness and decreasing velocity of the sedimentary layers can generate a reverberatory characteristic in the RFs (Yu et al., 2015). Therefore, larger sedimentary thicknesses can produce errors in the *H* results when applying the method described above. Thus, the conventional *H*-κ stacking procedure causes overestimates of *H* because the strong reverberations by multiple reflections (between the bottom of a loose sedimentary layer and the Earth's surface) associated with a low-velocity sedimentary layer can mask the Moho converted phases. In order to remove these effects of the sedimentary layers, we have applied the technique by Yu et al. (2015), which uses the arrival time of the P_xS phases and the two-way travel time of the sedimentary layers to correct the RFs (Figure 2). The removal of the reverberations clarifies the arrival of *Ps* from the Moho discontinuity (Figure 4). This procedure corrects the time delay and calculates the thicknesses of the unconsolidated sediment layer as well as the subsediment *H* and κ. Further details of the technique procedure are given by Yu et al. (2015).

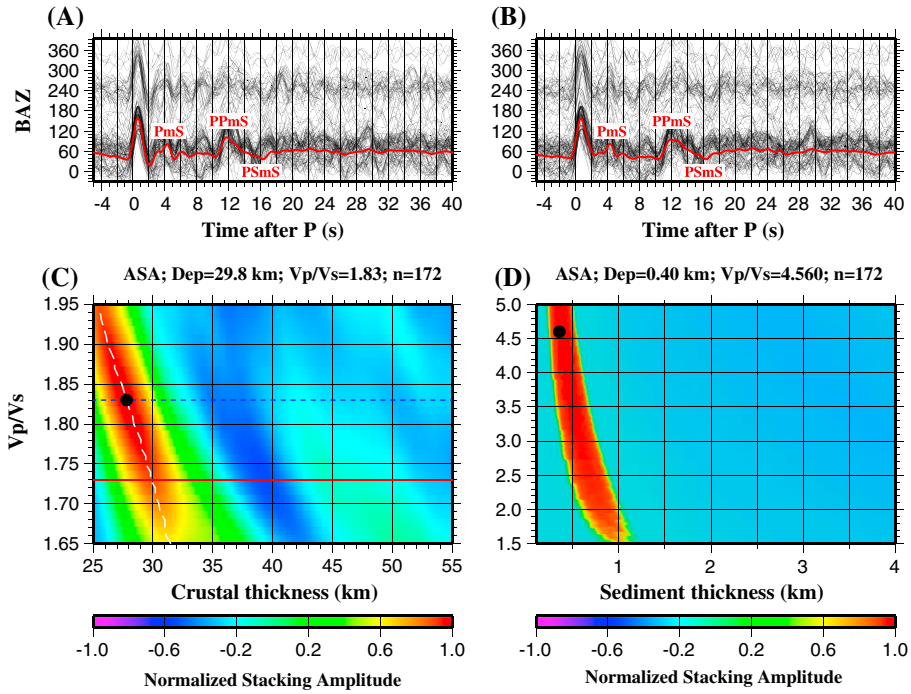

Figure 4. Application of *H*-κ plot for station ASA before and after the sediment correction, using the procedure of Yu et al. (2015). (a) Radial RFs plotted against the back azimuth, with a simple time series stack (red) before sediment moveout, (b) same as Figure 4a but after resource-removal filtering, and (c) *H*-κ grid plot for normalized stacking amplitude after the sediment moveout correction. The red line represents stacking amplitudes for $\kappa = 1.73$ (which is the mean κ for crustal rocks; Liu & Gao, 2010), the dashed blue line represents stacking amplitudes for the optimal κ and stacking amplitude along the dashed white. The optimal *H* and κ pair is indicated by a black dot. (d) Same as Figure 4c but for the *H*-κ grid plot for the stacking amplitude to determine sediment thickness.

On the other hand, an average *P* wave velocity of 3.5 km/s was used for the sedimentary layers during this study based on several studies related to oil surveys in Libya (e.g., Ben, 2000; Makris & Yegorova, 2006). The sediment velocity (3.5 km/s) for stacking would lead to an error of 0.024 km to 0.78 km in the resulting *H* value and 0.0052 to 0.13 in the resulting κ value. After the removal of the effects caused by the sedimentary layers, the amplitude of the first *Ps* phase from the base of the sedimentary layer (*PbS*) and the Moho phases appears more clearly (Figures 4–6).

3. Results

The values for *H* and κ for the crustal thickness and unconsolidated sediment layer thickness obtained from the 18 seismic stations are shown in Figures 7 and 8 and Tables 1 and 2. Each station was manually checked based on the displayed P_mS, as well as both the PP_mP and PS_mS arrivals. Figures 4–6 show an example from stations ASA, KFR, TATN, UMB, SHF, and JFR that display a clear arrival phase in a singular stacking point on the corresponding *H*-κ plot after the removal of effects from the sedimentary layers (some other examples from various seismic stations are given in Figures S1–S9 in the supporting information).

For the entire area of investigation, the resulting *H* values range from 24 km to 36 km, with a mean value of 32 km (with uncertainties ranging between ±0.10 km and ±0.90 km). The κ values range from 1.71 to 1.91, with a mean value of 1.83 (with uncertainties ranging between ±0.01 and ±0.04). The results suggest that the thinnest crust occurs mainly beneath the stations SRT, TRP, and JDB (Figure 7), whereas the thickest crust occurs beneath station KFR (the east central portion of the study area). In the coastal area, the *H* ranges from 24 km to 31 km, and the κ value ranges from 1.71 to 1.85. The northwestern part of the region is characterized by some of the lowest κ values, especially at stations GHAR and SRT (Figure 8). Stations GHD and ZLA (Figure S10 and S11) were not used in the study because of the very strong influence of a thick sedimentary layer that led to an approximately 1.5–2 s delay of the first *P* arrival on the radial RFs. The waveform does not have a dominant period; thus, the sedimentary removal procedure cannot be reliably applied in this case.

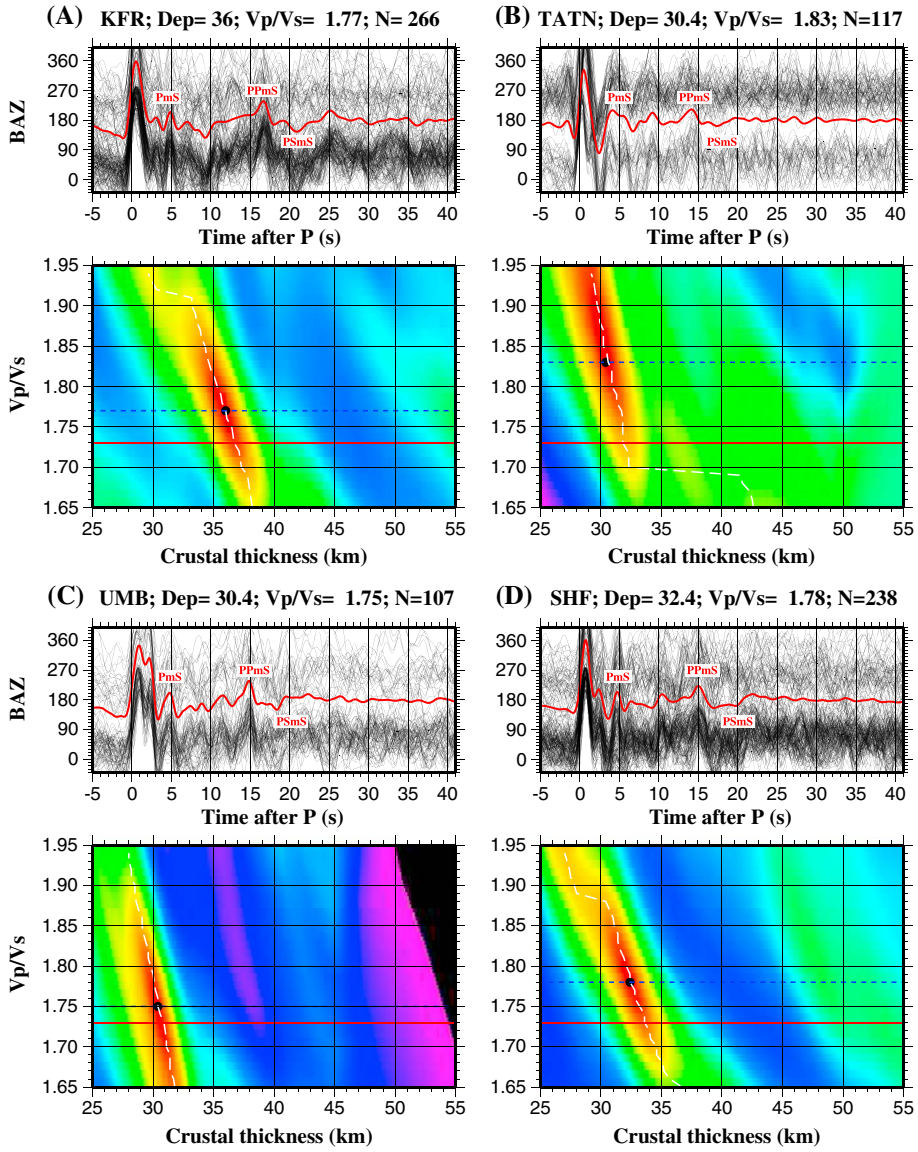

Figure 5. (a–d) Application of H-κ stacking for stations KFR, TATN, UMB, and SHF. The top panels show radial RFs (black) plotted against the back azimuth. The simple time domain summation of all the RFs that was recorded at the station is represented by the red line. The bottom panels are normalized amplitude grid with optimal H and κ pair indicated by a black dot. The red line represents stacking amplitudes for $\kappa = 1.73$, the dashed blue line represents stacking amplitudes for the optimal κ, and stacking amplitude along the dashed white.

Additionally, station TBQ was not used because it recorded an unreliable number of RFs (<10) (Figure S12). Our result for the stations GHAR and GHR shows that H is approximately 33 km, which is similar to the finding recorded by Van Der Meijde et al. (2003) who reported an average thickness of about 31 km.

To characterize the observed systematic spatial variations in the crust, we tested the correlations between crustal thickness, elevation, V_p/V_s, and Bouguer gravity anomalies for the region (Figure 9). We used a grid resolution for Bouguer gravity anomaly and elevation of 2 min and 1 min, respectively. Such resolutions are useful for large-scale geological studies and give critical information about the compensation mechanism of the Libyan territory (cf. Tontini et al., 2006). The H is directly proportional to the surface elevation with cross-correlation coefficient (r) of 0.55 (Figure 9a), and the H is inversely proportional to the Bouguer gravity anomaly with $r = -0.70$ (Figure 9c). We also compare the κ values with H, surface elevation, and Bouguer gravity anomaly and find no significant correlation with $r = -0.02$, -0.34, and 0.03, respectively (Figures 9e and 9f). We additionally observed a good correlation between elevation and Bouguer gravity anomalies

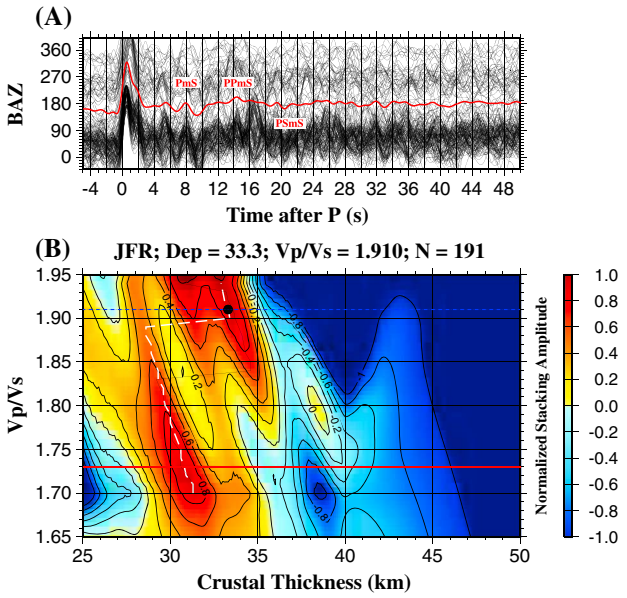

Figure 6. Same as Figure 5 but for station JFR at the AS Sawda Volcanic Province. Note that the κ value (1.91) most likely indicates partial melting beneath this region.

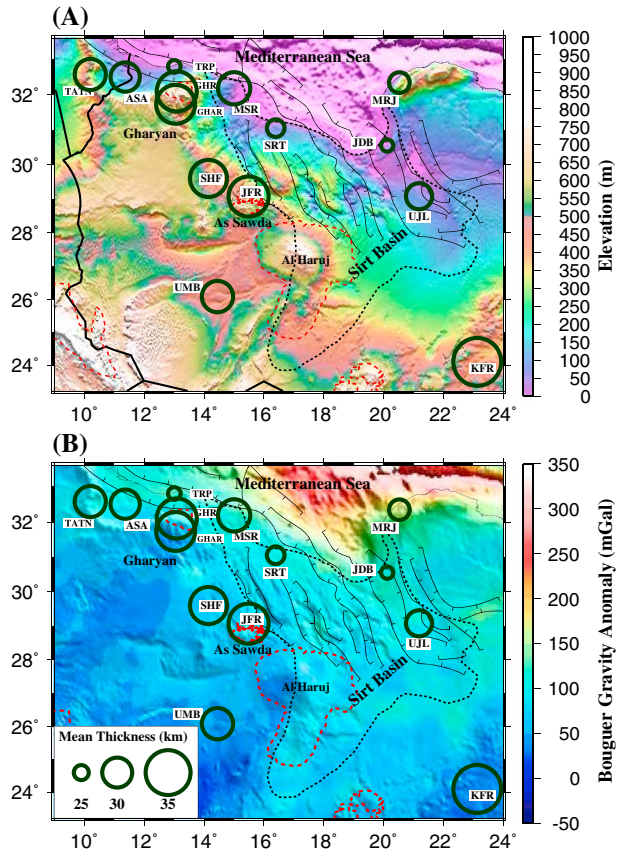

Figure 7. (a) Topographic relief map of the study area, with 1 min resolution, showing crustal thickness, and (b) resulting crustal thicknesses plotted on top of the Bouguer gravity map, which produced from the WGM2012 Bouguer gravity model with a resolution of 2 min. Note that circle diameter correlates with crustal thickness.

(r = 0.57) for 56 points where we picked up four measurements for both parameters at 2.5 km around each seismic station (Figure 9b). Hence, the greater surface elevations commonly correspond to the lower Bouguer anomalies and thicker crust, which may indicate an isostatically compensated crust.

Furthermore, applying the technique of Yu et al. (2015), as mentioned before, provides the sediment thickness beneath the stations in the study area. The sedimentary thickness ranges from 0.40 km to 3.70 km with κ values ranging from 1.50 to 4.80 (Table 2).

4. Discussion

4.1. Constraints on the Sediment Thickness

One of the drawbacks of using the receiver function technique is the existence of interferences resulting from sedimentary layers (Ammon, 1991; Langston, 1979; Owens et al., 1984; Zandt & Ammon, 1995; Zhu & Kanamori, 2000). Previously, some geophysical studies were conducted in the study area, especially along the coast, to estimate the thickness of the sedimentary layers using global velocity models (Cowie & Kusznir, 2012; Pasyanos & Nyblade, 2007). According to these previous studies, the thickness of these layers ranges from 1 to 7 km in the study area (e.g., Abadi et al., 2008). Hassan and Kendall (2014) summarized the geological and basin evolution in Libya, finding that the sediment thickness in the Sirt Basin varies from 1 km to 7 km; in the Murzuk Basin, it exceeds 4 km; in the Ghadamis Basin, it is about 7 km; in the Al Kufrah Basin, it is around 3 km; and in the northeast part of Libya, it varies from 3 km to 4 km.

This study find that the unconsolidated sediment layers beneath the seismic stations range from 0.40 km to 3.70 km, with κ ranging from 2.20 to 4.80. Anomalously high measurements of κ at some seismic stations might result from the presence of loose sediments, such as at stations ASA, JDB, MSR, and UJL (Table 2). Some seismic stations, such as stations TRP and SHF, show low κ values ranging from 2.20 to 3.0, suggesting that the areas beneath these stations have less compact sediments.

Due to the availability of seismic data, and the importance of oil, within the Sirt Basin region, we focus the discussion on this sedimentary basin. The results show that there is a significant change in the unconsolidated sediment layer thickness, ranging from 1.50 km to 2.20 km, the lowest value beneath stations UJL and MSR, and highest value at eastern boundary of the basin. This change may be related to extension within the basin and typeset of rocks. Furthermore, most of the previous studies (Abadi et al., 2008; Hassan & Kendall, 2014) did not consider the κ value of the sedimentary layers of the region. We have shown, as did Yu et al. (2015), that this is an important variable. The κ value in the Sirt Basin ranges from 3.50 to 4.80, which indicates that the sediments differ in their compactness. The technique that we used here did not work in some seismic stations, probably due to strong interfaces inside the sedimentary layer in the basins.

4.2. Crustal Composition, Pattern of Heat Flow, and Partial Melting Beneath Central Libya

The Cenozoic igneous rocks, which are exposed mainly in the central part of the region, comprise a low percentage of the region's surface geology (Suleiman, 1985). Geological studies (Al-Hafdh & El-Shaafi, 2015;

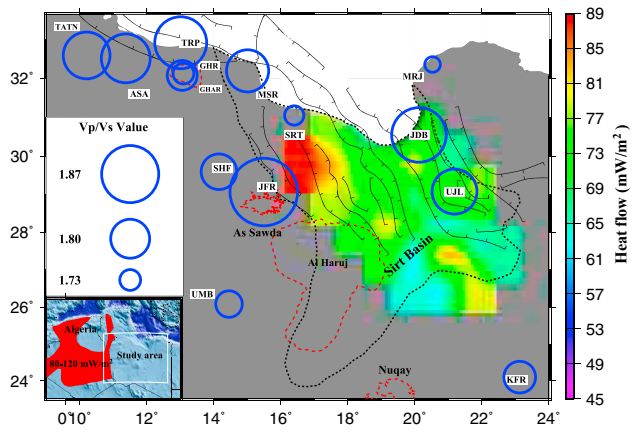

Figure 8. V_p/V_s values in the study area and patterns of heat flow across the Sirt Basin. The inset map shows the heat flow (80–120 mW/m^2) in the NW part of Africa at Algeria, which is indicated by a deep red color. The heat flow in the volcanic areas seems likely much higher than central and eastern parts of the Sirt Basin. The heat flow data are taken from Nyblade et al. (1996). Expanding circle diameters indicate increasingly κ values. The highest κ value (1.91) was recorded beneath the AS Swada Volcanic Province at station JFR. The main volcanic provinces represent by red dashed lines, and Mesozoic rifts represent by teeth on downthrown blocks (black lines).

Anketell, 1996; Cvetković et al., 2010; Klitzsch, 1971) suggest that the igneous rocks in these areas originated primarily from the partial melting of asthenospheric mantle materials.

Based on the classification of Holbrook et al. (1992), the crust composition in the study area is variable (Figure 8), with small κ values (1.72 to 1.77) occurring beneath stations SRT, UMB, and KFR, indicative of felsic rocks. For other stations, the values range from 1.80 to 1.86 and are indicative of intermediate rocks, except for station JFR, where a value above 1.86 suggests mafic rocks. In addition, Watanabe (1993) interpreted rapid reduction of V_s relative to V_p, the κ value, as being a function of melt percentage, the melt being primarily noticeable for values above 1.86. Reed et al. (2014) inferred that the high κ (>1.86) beneath the Red Sea rift and adjacent regions indicates widespread partial melting. The observed low values of V_s are interpreted as reflecting present-day thermal effects within the central part of Libya (cf. Begg et al., 2009; Deen et al., 2006).

Overall, the crustal composition in the study area is intermediate to mafic. In the volcanic and coastal areas, κ values are high, especially at stations JFR, TATN, JDB, ASA, and TRP. This indicates that the crustal composition beneath these stations is predominantly mafic. Other κ values suggest that the crustal composition is mainly intermediate. Our observations of velocities obtained from seismic stations at the volcanic provinces (SHF, JFR, and GHR) broadly agree with other geochemical and petrological studies on the composition of crustal materials (e.g., Aboazom et al., 2006; Al-Hafdh & El-Shaafi, 2015; Al-Hafdh & Gafeer, 2015).

As discussed by Abdelsalam et al. (2002) and Lemnifi et al. (2015) a negative of shear wave velocity at depth of 100–175 km reflects the delamination of a cratonic root. This is in agreement with our results, especially from data obtained from stations KFR and UMB (Figures 5a and 5c), which give values of κ ranging between 1.75 and 1.77, respectively. The κ values are not high enough to indicate partial melt beneath the lower crust or delamination process beneath the Al Kufra and Murzuk Basins. However, these values may indicate that heat flux beneath the base of the lower crust is not high or, alternatively, the values may be an effect of the thickness in this part of Libyan territory.

Table 1
Observations of Crustal Thickness (H) and V_p/V_s (κ)

Station	Latitude (deg)	Longitude (deg)	N	H (km)	V_p/V_s (κ)	Rank
ASA	32.51	11.37	172	29.8 ± 0.37	1.83 ± 0.01	A
GHAR	32.12	13.10	41	33.4 ± 0.80	1.73 ± 0.03	A
GHR	32.07	13.05	203	33.0 ± 0.12	1.76 ± 0.01	A
JDB	30.55	20.12	11	24.10 ± 0.00	1.86 ± 0.00	B
JFR	29.06	15.49	191	33.30 ± 0.12	1.91 ± 0.01	A
KFR	24.10	23.13	266	36.0 ± 0.19	1.77 ± 0.00	A
MRJ[a]	32.35	20.53	60	27.0 ± 0.28	1.71 ± 0.03	A
MSR	32.19	15.01	184	30.90 ± 0.26	1.81 ± 0.01	A
SHF	29.59	14.15	238	32.37 ± 0.21	1.78 ± 0.01	A
SRT	31.05	16.39	80	26.10 ± 0.44	1.72 ± 0.04	B
TANT	32.58	10.53	117	30.40 ± 0.58	1.83 ± 0.02	A
TRP	32.51	13.10	32	24.20 ± 0.79	1.85 ± 0.02	B
UJL	29.07	21.18	149	28.80 ± 0.16	1.82 ± 0.01	A
UMB	26.08	14.45	107	30.44 ± 0.13	1.75 ± 0.01	A

[a]Merged two stations.

Table 2
Observations of Sediment Thickness (H), and V_p/V_s (κ)

Station	Latitude (deg)	Longitude (deg)	N	H (km)	V_p/V_s (κ)	Rank
ASA	32.51	11.37	172	0.40 ± 0.02	4.56 ± 0.13	A
JDB	30.55	20.12	6	2.17 ± 0.06	4.21 ± .08	B
MSR	32.19	15.01	184	0.80 ± 0.26	4.79 ± 0.01	A
SHF	29.59	14.15	238	1.90 ± 0.21	2.29 ± 0.01	A
SRT	31.05	16.39	80	2.00 ± 0.44	3.48 ± 0.04	B
TRP	32.51	13.10	32	3.70 ± 0.79	2.21 ± 0.02	A
UJL	29.07	21.18	149	1.50 ± 0.16	4.75 ± 0.01	A

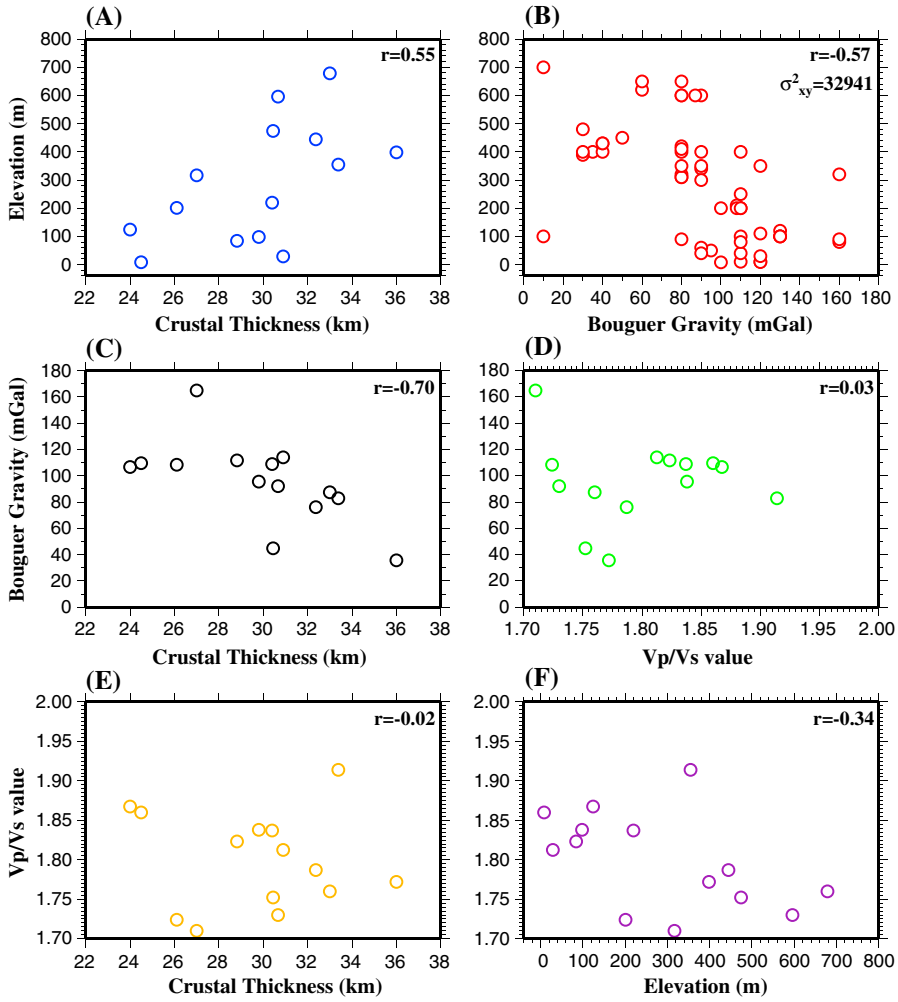

Figure 9. Graphs showing the correlations between crustal thickness, elevation, Bouguer Gravity, and V_p/V_s. (a) Correlation between crustal thickness and elevation with $r = 0.55$ where r is the cross-correlation coefficient. (b) Correlation between Bouguer gravity anomaly and elevation with $r = -0.57$, $\sigma^2(x, y) = 32,941$, where $\sigma(x, y)$ is the sum of variance elevation (x) plus Bouguer gravity anomaly (y) due to both x and y are correlated. (c) Correlation between crustal thickness and Bouguer gravity anomaly with $r = -0.70$. (d) Correlation between Bouguer gravity anomaly and V_p/V_s values with $r = 0.03$. (e) Correlation between crustal thickness and V_p/V_s values with $r = -0.02$. (f) Correlation between elevation and V_p/V_s values with $r = -0.34$.

Heat flow across the Sirt Basin has been shown to be normal to slightly elevated (49–91 mW m^2) and generally higher in platforms (horsts) than grabens (Figure 8) (Nyblade et al., 1996). It has been suggested that the heat flow in the Sirt Basin is too low, particularly compared with that of the Sahara basins (northwestern Africa), to support the idea of a lithospheric thermal anomaly (Nyblade et al., 1996). Heat flow measurements suggest that the elevated heat flow is primarily concentrated in the western part of the Sirt Basin (77–91 mW m^2) in areas close to the Al Haruj and AS Sawda Volcanic Provinces (Nyblade et al., 1996) (Figure 8). In addition, maturation depth trends in the western Sirt Basin are higher than in the eastern and central parts, suggestive of elevated paleogeothermal gradients in the late Cenozoic (up to 30°C/km) (Abadi et al., 2008; Gumati & Schamel, 1988). It is thus likely that elevated heat flow in the western Sirt Basin is related to enhanced crustal heat production rather than to thermal alteration of the lithosphere related to rifting of the Sirt Basin (Nyblade et al., 1996) (Figure 8). However, a lack of heat flow data prevents a precise evaluation of heat flow in the northwestern part of Africa between Algeria and the Sirt Basin (Figure 8). In these regions the heat flow in volcanic areas, such as the western part of the Sirt Basin, are indeed likely to be much higher than central and eastern parts of the Sirt Basin.

The high κ values show velocity ratios suggesting the presence of fluids and melts (Deen et al., 2006; Reed et al., 2014; Watanabe, 1993). The κ values in the volcanic regions throughout Libyan territory are significantly greater than those found in other areas, particularly at the JFR station (AS Sawda Volcanic Province) (1.91) (Figure 6). These values are significantly greater than those found in other areas. This suggests the existence of partial melt within the crust beneath the volcanic areas. The modern-age dating for the last volcanic phase at the Al Haruj Volcanic Province, central Libya, indicates ages as young as 2.3 $\pm$ 0.8 ka (Nixon et al., 2011), indicating that the magma reservoir beneath this volcanic field is still active (Elshaafi & Gudmundsson, 2017a). In addition, the Al Haruj and Waw an Namous volcanic fields in central Libya (Figure 1) are considered as still potentially volcanically active (Bardintzeff et al., 2012; Siebert & Simkin, 2002).

Isotope data and geochemical signatures for basaltic rocks within the Al Haruj Volcanic Province indicate that fractional crystallization of primitive magma took place at depths of 25–39 km and temperatures of 1215–1360°C (Nixon et al., 2011). The majority of earthquakes in Libya occur at depths around 30–35 km (Al-Heety, 2013) that suggests that the increased seismogenic thickness in Libya corresponds to a thick lithosphere underlying the region (cf. Craig et al., 2011; Priestley & McKenzie, 2006). The depths of the proposed magma reservoirs and the earthquakes coincide with the depths that our results give for the Moho. The results suggest that the proposed magma reservoirs at the Al Haruj and AS Sawda Volcanic Provinces could be located in the transition zone between the lowermost crust and the upper mantle. Results from other volcanic areas, such as Iceland, suggest that many partially molten magma reservoirs tend to be located at the boundary between the upper mantle and the lower crust (Elshaafi & Gudmundsson, 2017a; Gudmundsson, 1986, 2016; cf. Hermance, 1981; Schmeling, 1985).

Magma reservoirs at the contact between the upper mantle and the lower crust can remain active for millions of years or more and mantle plumes exist for tens of millions of years, particularly when located away from plate boundaries (Courtillot et al., 2003; Elshaafi & Gudmundsson, 2017b; Gudmundsson et al., 2009, 2016) as in the present case. Consequently, the magma reservoirs beneath parts of Libya, particularly the central part (at Al Haruj, Waw an Namous and AS Sawda volcanic fields), are likely to be still active. In which case, mechanical interaction is possible over the same time spans as the magma chamber/reservoir acts to concentrate stress (Andrew & Gudmundsson, 2008; Biggs et al., 2016; Elshaafi and Gudmundsson, 2017b). The magma reservoirs beneath the Libyan territory would contribute to the generation of zones of tensile and shear stresses within and in-between these volcanic provinces. The concentration of elevated stresses poses a significant earthquakes and volcanic hazard (for more details see Elshaafi & Gudmundsson, 2017b).

4.3. Libyan Continental Interior and Coastal Area Crustal Thickness

The *H* varies spatially throughout Libya, with the northern central portion having the thinnest crust and the interior having the thickest crust. Most of the seismic stations located along the uplifted areas, such as stations JFR and GHAR (Figure 7), suggest *H* of >32 km. From these thicknesses we deduce that uplift occurred in this area and volcanic activity played a contributing role in the determining *H* and composition. Results for *H* and κ represent aspects of crustal formation and evolution as illustrated in Figures 7 and 8.

The crust beneath the central and northwestern parts of Libya is as much as 5 km thinner than in the southeast and southwest parts. It is widely agreed (e.g., Faccenna et al., 2001; Marone et al., 2003) that the *H* might relate

to the opening of the Paleozoic ocean to the north (Granot, 2016) and the heterogeneity of tectonic processes in the area.

4.4. Comparing Crustal Thickness With Elevation and Bouguer Gravity Anomalies

The question then arises: is the crust in Libya compensated only by isostasy or instead by mantle dynamics? Numerous studies have discussed the relationship between gravity anomalies and H (e.g., Aiken, 1976; Assumpcáo et al., 2013; Bashir et al., 2011; Hendricks & Plescia, 1991; Sumner, 1989). We tested correlations between H, elevation, and Bouguer gravity anomalies (Figure 9) and found that they are correlated.

The studies by Egorkin (1998) and Zandt and Ammon (1995) indicate that geological processes of different ages can be distinguished by their relation of H and κ values. But our results do not support these suggestions since we find a weak correlation between H and κ values with $r = -0.02$ in the region (Figure 9e).

A number of previous studies (e.g., Boschi et al., 2010; Flament, 2014; Forte et al., 1993, 2010; Gurnis, 1993; Husson et al., 2014; Lithgow-Bertelloni & Silver, 1998; Liu & Gurnis, 2010; Moucha & Forte, 2011; Moucha et al., 2009) propose that surface elevations of >1 km are mainly controlled by mantle convention. Long-wavelength dynamic topography can account for topography smaller than 500 m, which supports the idea that surface topography can be created by mantle convection, whereas short wavelengths can be related to local thermal settings (Hoggard et al., 2016). In Libya, surface elevations are <500 m except in some volcanic provinces where the surface elevation reaches above 850 m. We suggest that these elevation differences at volcanic areas are supported by mantle convection, which supports the findings of several previous studies (e.g., Hoggard et al., 2016). According to the correlation between surface elevation and H, we propose that the crust is isostatically compensated. It has been suggested that the crust near/within adjacent areas to the Eurasia-Africa plate boundary region are in close-to-isostatic equilibrium (Marone et al., 2003). The results show that the crust is 30–36 km thick throughout the high elevation parts of the interior of Libya but much thinner, 24–28 km, under the lower topography parts along the coastal area, except in the northwest at the Gharyan Volcanic Province.

The available seismic data are still limited for explore the detailed relationships between elevation, crustal thickness, and the Bouguer anomalies. However, data from this analysis indicate a crustal thickness variation that is in agreement with studies by Assumpcáo et al. (2013), Oliveira and Medeiros (2012), and Van Der Meijde et al. (2013), who estimated the H using modeling gravimetric anomalies. The results thus indicate that the Moho depth might constrain the topography of Libya, as suggested in Brazil region (e.g., Assumpcáo et al., 2013; Feng et al., 2007; Lloyd et al., 2010). The correlations in Figure 9 suggest an isostatically compensated crust: higher elevations correspond to lower Bouguer anomalies and thicker crust. Using the Airy model to crudely calculate the density of the crust beneath the study area, we find it to be approximately 3,140 kg/m^3, which is above the average found using typical values of crustal density (2,850 kg/m^3 to 2,880 kg/m^3) (e.g., Darbyshire et al., 2000; Woollard, 1959) and lower than densities derived from Makris and Vees (1977), Makris and Stobbe (1984), and Makris and Yegorova (2006), which are 3,300 kg/m^3. Therefore, we propose that the crust beneath Libya is old and dense, possibly having been formed during the Precambrian to Early Paleozoic age, which agree with the finding by Granot (2016) and Speranza et al. (2012) beneath the eastern Mediterranean Sea. Meanwhile, results of surface wave modeling by Fishwick (2010), who observed the thinner lithosphere beneath central Libya and delamination of cratonic roots beneath Sahara metacraton (Abdelsalam et al., 2011), tend to support the idea that the area is under isostatic equilibrium. As such, the thinner lithosphere can lead to the rise of the asthenosphere and promote isostatic equilibrium, which leads to local mountain building. This follows because although volcanic eruptions during the late Cenozoic period supplied mafic magmas to the underlying crust in some areas, hence the idea of having a dense crust suggests a poor correlation between Bouguer gravity anomalies and κ ratios, with r of 0.03 (Figure 9d) and inverse correlation between topography and Bouguer gravity anomalies (Figure 9b). However, the crustal thickness shows a good reverse relation with Bouguer gravity anomalies, which supports the assumption of an older origin for the overall denser crust.

Crustal thickness has been shown to vary significantly in the East Saharan Shield area depending on the models used (e.g., Bassin et al., 2000; Pasyanos & Nyblade, 2007). The Pasyanos and Nyblade (2007) velocity model gives H ranging from 25 to 35 km, while CRUST2.0 (Bassin et al., 2000) indicates crustal ranging from 35 km to 45 km. Results from this study agree closely with the more recent of the two studies yielding an overall denser crust, since such a crust would also have higher velocities.

Crustal uplifts are generally interpreted as hot spot swells because association with intraplate volcanism and large gravity anomalies (Pirajno, 2004). However, the spatial distributions of Libya's volcanism have also been related to a warm upwelling asthenospheric mantle associated with a thinner lithosphere that promotes magma migration through metasomatized lithospheric channels (Ball et al., 2016; Elshaafi & Gudmundsson, 2017a; Nixon et al., 2011). Furthermore, a low-density anomaly sits beneath the lithospheric plate and Libya's volcanic provinces are distinguished by a series of long-wavelength topographic swells (Ball et al., 2016).

The major volcanic fields in Libyan territory are greatly correlated to the current elevated basement areas. The basement highs seem to reflect some form of subcrustal arching rather than magmatic intraplate accumulation as inferred from isotope geochemical data that indicate that the magmas lack signals of crustal contamination and, hence, most likely magma propagated directly from deep-seated magma reservoirs at the crust-mantle boundary (Elshaafi & Gudmundsson, 2017a; Stuart et al., 2014). There are no large igneous bodies such as extensive sills observed in seismic lines in the western part of the Sirt Basin (e.g., Abdunaser & McCaffrey, 2015). Hence, the lack of large plutonic bodies or extinct shallow magma chambers beneath the Earth's crust may be one reason for the low Bouguer anomaly in volcanic areas as observed in this study. It is generally accepted that a hot upwelling mantle induces dynamic uplift (Courtillot et al., 2003; Pirajno, 2004) where the impact of a mantle plume onto the base of the lithosphere results in doming of the crust. The dynamic topography is quite difficult to determine in the continents, particularly in Africa, due to the density structure of the lithosphere, which is still unknown and poorly documented (cf. Ball et al., 2016). Further geophysical studies such as heat flow data, denser broadband seismic coverage, and geothermal data should be addressed in the future in order to obtain better constraints on the deep structure and density of the lithosphere beneath this important region.

5. Conclusions

This is the first study to present H measurements of Libya based on seismic data obtained from a large number of seismic stations. The H ranges from 24 km to 36 km. More specifically, the range in H is from a maximum of 30–36 km beneath the southern part of Libya to a minimum of 24–28 km along its coast. We find a significant correlation between H, elevation, and Bouguer gravity, suggesting that the crust is isostatically compensated. However, there is a weak correlation between H and κ values. The main volcanic provinces in Libya mostly coincide with the current elevated areas and low Bouguer gravity anomalies, which indicates that the volcanic regions have been subject to subcrustal arching rather than magmatic underplating. This study observe that seismic stations close to volcanic provinces detect more mafic crustal compositions because of basaltic magma underlying the crust, possibly forming partially molten magma reservoirs. The value at station JRF is 1.91, suggesting the existence of partial melt at the crust-mantle boundary beneath the associated volcanic field. Modern age dating by Nixon et al. (2011) at the Al Haruj Volcanic Province indicates that the volcanism in this region continued until recent times. If magma resides beneath central Libya in reservoirs, then the volcanic systems may pose a significant earthquake and volcanic risks. Many earthquakes that occurred in Libya during the past century have depths between 30 km and 35 km (Al-Heety, 2013). Fractional crystallization of the primitive magmas at the Al Haruj Volcanic Province is also thought to have occurred at similar depths, namely, in reservoirs at depths of 25–39 km (Nixon et al., 2011). The inferred depths of the reservoirs coincide our findings of Moho depth variations. This study also find that sediment thicknesses beneath the seismic stations range from 0.4 km to 3.7 km, with variable values of κ. Using an Airy isostasy model suggests that the density of the crust beneath the study area is 3,140 kg/m^3. We suggest that the crust in this region is denser than normal and therefore likely to be older than Phanerozoic time.

Acknowledgments

Data used in this study were obtained from two sources: (1) Libyan Center for Remote Sensing and Space Science (LCRSSS) and (2) the IRIS DMC. We are grateful to Y. Yu for assistance with data processing and S. Gao for helpful discussions and comments. We thank C. Reed for providing Bouguer gravity anomaly data for Figure 7b, as well as A. A. Elmelade for providing seismic data from the LCRSSS. We thank the Editors U. ten Brinkand and D. van Hinsbergen and two anonymous reviewers for their constructive comments that helped to improve an earlier version of the manuscript. We are grateful for support from the Benghazi University of Libya. Also, this study was partially supported by Mining Engineering Department, Missouri University of Science and Technology, Rolla, Missouri, USA. All the receiver functions used in the study can be found in the supporting information section. The RFs are in SAC (Seismic Analysis Codes) format. Also included in the supporting information section are a catalog of earthquakes used, as well as an H-κ plot for each of the stations.

References

Abdelsalam, M. G., Gao, S. S., & Liégeois, J. P. (2011). Upper mantle structure of the Saharan Metacraton. *Journal of African Earth Sciences*, *60*(5), 328–336. https://doi.org/10.1016/j.jafrearsci.2011.03.009

Abdelsalam, M. G., Liégeois, J. P., & Stern, R. J. (2002). The Saharan Metacraton. *Journal of African Earth Sciences*, *34*, 119–136. https://doi.org/10.1016/S0899-5362(02)00013-1

Abadi, A., van Wees, J., van Dijk, P., & Cloetingh, S. (2008). Tectonics and subsidence evolution of the Sirt Basin, Libya. *Bulletin-American Association of Petroleum Geologists*, *92*, 993–1027. https://doi.org/10.1306/03310806070

Abdunaser, K, & McCaffrey, K. (2015). Tectonic history and structural development of the Zallah-Dur al Abd sub-basin, western Sirt Basin, Libya. *Journal of Structural Geology*, *73*, 33–48. https://doi.org/10.1016/j.jsg.2015.02.006

Aboazom, A. S., Asran, A. S. H., Abdel Ghani, M. S., & Farhat, E. S. (2006). Geologic and geochemical constraints on the origin of some Tertiary alkaline rift volcanics, Gharyan area, northwestern Libya. *Journal of Geology*, *35*, 25–47.

Aiken, C. (1976). The analysis of the gravity anomalies of Arizona (PhD dissertation), University of AZ, Tucson.

Al-Hafdh, N. M., & El-Shaafi, A. S. (2015). Geochemistry and petrology of basic volcanicrocks of Jabal Al Haruj Al-Aswad, Libya. *International Journal of Geosciences*, *6*, 109–144. https://doi.org/10.4236/ijg.2015.61008

Al-Hafdh, N. M., & Gafeer, A. S. (2015). The petrology and geochemistry of Gharyan Volcanic Province of NW Libya. *Journal of African Earth Sciences*, *104*, 71–102. https://doi.org/10.1016/j.jafrearsci.2014.11.006

Al-Heety, E. (2013). Seismicity and seismotectonics of Libya: As an example of intraplate environment. *Arabian Journal of Geosciences*, *6*, 193–204. https://doi.org/10.1007/s12517-011-0347-y

Ammon, C. J. (1991). The isolation of receiver effects from teleseismic *P* waveforms. *Bulletin of the Seismological Society of America*, *81*, 2504–2510.

Andrew, R., & Gudmundsson, A. (2008). Volcanoes as elastic inclusions: Their effects on the propagation of dykes, volcanic fissures, and volcanic zones in Iceland. *Journal of Volcanology and Geothermal Research*, *177*, 1045–1054. https://doi.org/10.1016/j.jvolgeores.2008.07.025

Anketell, J. M. (1996). Structural history of Sirt Basin and its relationship to the Sabratah Basin and Cyrenaica platform, northern Libya. In M. J. Salem et al. (Eds.), *The Geology of sirt basin* (Vol. 3, pp. 57–89). Amsterdam: Elsevier.

Assumpcáo, M., Bianchi, M., Juliá, Dias, F. L., Frana, G. S., Nascimento, R., … Lopes, A. E. V. (2013). Crustal thickness map of Brazil: Data compilation and main features. *Journal of South American Earth Sciences*, *43*, 74–85. https://doi.org/10.1016/j.jsames.2012.12.009

Ball, P. N., White, N. J., Maclennan, J., & Stuart, F. (2016). Magmatism and Dynamic Topography of Libya and Tibesti, North Africa, American Geophysical Union, Fall General Assembly, Abstract DI51B-2667.

Bardintzeff, J. M., Deniel, C., Guillou, H., Platevoet, B., Tćlouk, P., & Oun, K. H. (2012). Miocene to recent alkaline volcanism between Al Haruj and Waw an Namous (southern Libya). *International Journal of Earth Sciences*, *101*, 1047–1063. https://doi.org/10.1007/s00531-011-0708-5

Bashir, L., Gao, S. S., Liu, K. H., & Mickus, K. (2011). Crustal structure and evolution beneath the Colorado Plateau and the southern Basin and Range Province: Results from receiver function and gravity studies. *Geochemistry, Geophysics, Geosystems*, *12*, Q06008. https://doi.org/10.1029/2011GC003563

Bassin, C., Laske, G., & Masters, G. (2000). The current limits of resolution for surface wave tomography in North America. *Eos Transactions American Geophysical Union*, *81*, F897.

Begg, G. C., Griffin, W. L., Natapov, L. M., O'Reilly, S. Y., Grand, S. P., O'Neill, C. J., … Bowden, P. (2009). The lithospheric architecture of Africa: Seismic tomography, mantle petrology, and tectonic evolution. *Geosphere*, *5*, 23–50. https://doi.org/10.1130/GES00179.1

Ben, S. A. (2000). Hydrocarbon prospectivity to the north-west of the assumoodeld, Sirt Basin, Libya (Durham theses), (http://etheses.dur.ac.uk/4379/). Durham University.

Biggs, J., Robertson, E., & Cashman, K. (2016). The lateral extent of volcanic interactions during unrest and eruption. *Nature Geoscience*, *9*, 308–311. https://doi.org/10.1038/ngeo2658

Boschi, L., Faccenna, C., & Becker, T. W. (2010). Mantle structure and dynamic topography in the Mediterranean Basin. *Geophysical Research Letters*, *37*, L20303. https://doi.org/10.1029/2010GL045001

Capitanio, F. A., Faccenna, C., & Funiciello, R. (2009). The opening of Sirte Basin: Result of slab avalanching? *Earth and Planetary Science Letters*, *285*, 210–216. https://doi.org/10.1016/j.epsl.2009.06.019

Christensen, N. I. (1996). Poisson's ratio and crustal seismology. *Journal of Geophysical Research*, *101*, 3139–3156. https://doi.org/10.1029/95JB03446

Christensen, N. I., & Mooney, W. D. (1995). Seismic velocity structure and composition of the continental crust: A global view. *Journal of Geophysical Research*, *100*, 9761–9788. https://doi.org/10.1029/95JB00259

Clarke, T. J., & Silver, P. G. (1993). Estimation of crustal Poisson's ratio from broadband teleseismic data. *Geophysical Research Letters*, *20*, 241–244. https://doi.org/10.1029/92GL02922

Courtillot, V., Davaille, A., Besse, J., & Stock, J. (2003). Three distinct types of hotspots in the Earth's mantle. *Earth and Planetary Science Letters*, *205*, 295–308. https://doi.org/10.1016/S0012-821X(02)01048-8

Cowie, L., & Kusznir, N. (2012). Gravity inversion mapping of crustal thickness and lithosphere thinning for the Eastern Mediterranean. *The Leading Edge*, *31*, 810–814. https://doi.org/10.1190/tle31070810.1

Craig, J., Jackson, J., Priestley, A., & McKenzie, D. (2011). Earthquake distribution patterns in Africa: Their relationship to variations in lithospheric and geological structure, and their heological implications. *Geophysical Journal International*, *185*, 403–434. https://doi.org/10.1111/j.1365-246X.2011.04950.x

Craig, J., Rizzi, C., Said, F., Thusu, B., Luning, S., Asbali, A., … Hamblett, C. (2008). Structural styles and prospectivity in the Precambrian and Palaeozoic hydrocarbon systems of North Africa. In M. J. Salem, K. M. Oun, & A. S. Essed (Eds.), *The Geology of East Libya* (Vol. 4, pp. 51–122). Earth Science Society of Libya.

Cvetković, V., Toljić, M., Ammar, N. A., Rundić, L., & Trish, K. B. (2010). Petrogenesis of the eastern part of the Al Haruj basalts (Libya). *Journal of African Earth Sciences*, *58*, 37–50.

Deen, T., Griffin, W. L., O'Reilly, G., Begg, S. Y., & Natapov, L. M. (2006). Thermal and compositional structure of the subcontinental lithospheric mantle: Derivation from shear-wave seismic tomography. *Geochemistry, Geophysics, Geosystems*, *7*, Q07003. https://doi.org/10.1029/2005GC001164

Darbyshire, F. A., White, R. S., & Priestley, K. F. (2000). Structure of the crust and uppermost mantle of Iceland from a combined seismic and gravity study. *Earth and Planetary Science Letters*, *181*, 409–428. https://doi.org/10.1016/S0012-821X(00)00206-5

Doucoure, C. M., & de Wit, M. J. (2003). Old inherited origin for the present near-bimodal topography of Africa. *Journal of African Earth Sciences*, *36*, 371–388. https://doi.org/10.1016/S0899-5362(03)00019-8

Ebinger, C. J., & Sleep, N. H. (1998). Cenozoic magmatism throughout East Africa resulting from impact of a single plume. *Nature*, *395*, 788–791. https://doi.org/10.1038/27417.

Efron, B., & Tibshirani, R. (1986). Bootstrap methods for standard errors, confidence intervals, and other measures of statistical accuracy. *Statistical Science*, *1*, 54–77.

Egorkin, A. V. (1998). Velocity structure, composition and discrimination of crustal provinces in the former Soviet Union. *Tectonophysics*, *298*, 395–404. https://doi.org/10.1016/S0040-1951(98)00192-9

Elshaafi, A., & Gudmundsson, A. (2016). Volcano-tectonics of the Al Haruj Volcanic Province, central Libya. *Journal of Volcanology and Geothermal Research*, *325*, 189–202. https://doi.org/10.1016/j.jvolgeores.2016.06.025

Elshaafi, A., & Gudmundsson, A. (2017a). Distribution and size of lava shields on the Al Haruj al Aswad and the Al Haruj al Abyad volcanic systems, central Libya. *Journal of Volcanology and Geothermal Research*, *338*, 46–62. https://doi.org/10.1016/j.jvolgeores.2017.03.012

Elshaafi, A., & Gudmundsson, A. (2017b). *Mechanical interaction between volcanic systems in Libya*, Tectonophysics, https://doi.org/10.1016/j.tecto.2017.11.031

Faccenna, C., Funiciello, F., Giardini, D., & Lucente, P. (2001). Episodic backarc extension during restricted mantle convection in the central Mediterranean. *Earth and Planetary Science Letters*, *187*, 105–116. https://doi.org/10.1016/S0012-821X(01)00280-1

Feng, M., Van Der Lee, S., & Assumpçã, M. (2007). Upper mantle structure of South America from joint inversion of waveforms and fundamental-mode group velocities of Rayleigh waves. *Journal of Geophysical Research*, *112*, B04312. https://doi.org/10.1029/2006JB004449

Fishwick, S. (2010). Surface wave tomography: Imaging of the lithosphere-asthenosphere boundary beneath central and southern Africa? *Lithos*, *120*(1), 63–73. https://doi.org/10.1016/j.lithos.2010.05.011

Flament, N. (2014). Linking plate tectonics and mantle flow to Earth's topography. *Geology*, *42*, 927–928. https://doi.org/10.1130/focus102014.1

Forte, A. M., Peltier, W. R., Dziewonski, A. M., & Woodward, R. L. (1993). Dynamic surface topography: A new interpretation based upon mantle flow models derived from seismic tomography. *Geophysical Research Letters*, *20*, 225–228. https://doi.org/10.1029/93GL00249.

Forte, A. M., Quéré, S., Moucha, R., Simmons, N. A., Grand, S. P., Mitrovica, J. X., & Rowley, D. B. (2010). Joint seismic-geodynamic-mineral physical modeling of African geodynamics: A reconciliation of deep mantle convection with surface geophysical constraints. *Earth and Planetary Science Letters*, *295*, 329–341. https://doi.org/10.1016/j.epsl.2010.03.017

Granot, R. (2016). Palaeozoic oceanic crust preserved beneath the Eastern Mediterranean. *Nature Geoscience*, *9*, 701–705. https://doi.org/10.1038/ngeo2784

Griffin, W., & O'Reilly, S. (1987). Is the continental Moho the crust-mantle boundary? *Geology*, *15*, 241–244. https://doi.org/10.1130/0091-7613(1987)15<241:ITCMTC>2.0.CO;2

Gudmundsson, A. (1986). Mechanical aspects of postglacial volcanism and tectonics of the Reykjanes Peninsula, southwest Iceland. *Journal of Geophysical Research*, *91*, 12711–12721.

Gudmundsson, A. (2016). The mechanics of large volcanic eruptions. *Earth-Science Reviews*, *163*, 72–93. https://doi.org/10.1016/j.earscirev.2016.10.003.

Gudmundsson, A., Friese, N., Andrew, R., Phillpp, S. L., Ertl, G., & Letourneur, L. (2009). Effects of dyke emplacement and plate pull on mechanical interaction between volcanic systems and central volcanoes in Iceland. In T. Thordarson et al. (Eds.), *Studies in volcanology: The legacy of George Walker, Special Publication of IAVCEI* (Vol. 2, pp. 331–347). London, UK: Geological Society.

Guiraud, R., & Bosworth, W. (1997). Senonian basin inversion and rejuvenation of rifting in Africa and Arabia: Synthesis and implications to plate-scale tectonics. *Tectonophysics*, *282*, 39–82. https://doi.org/10.1016/S0040-1951(97)00212-6

Gumati, Y., & Schamel, S. (1988). Thermal maturation history of the Sirte Basin, Libya. *Journal of Petroleum Geology*, *11*, 205–218. https://doi.org/10.1111/j.1747-5457.1988.tb00814.X

Gurnis, M. (1993). Phanerozoic marine inundation of continents driven by dynamic topography above subducting slabs. *Nature*, *364*, 589–593. https://doi.org/10.1038/364589a0

Hassan, H. S., & Kendall, C. G. (2014). Hydrocarbon provinces in Libya: A petroleum system study. In L. Marlow et al. (Eds.), *Petroleum systems of the Tethyan region* (Vol. 106, pp. 101–142). London: Geological Society Special Publication.

Hegazy, A. H. (1999). *Tertiary volcanics in Libya: Evidence for the direction and rate of the African plate motion*, paper presented at Proceeding of the 4th International Conference on Geochemistry, (pp. 401–419). Egypt: Alexandria University.

Hendricks, J. D., & Plescia, J. B. (1991). A review of the regional geophysics of the Arizona transition zone. *Journal of Geophysical Research*, *96*, 12,351–12,373. https://doi.org/10.1029/90JB01781

Hermance, J. (1981). Crustal gensis in Iceland: Geophysical constraints on crustal thickening with age. *Geophysical Research Letters*, *8*, 203–206. https://doi.org/10.1029/GL008i003p00203

Hoggard, M. J., White, N. J., & Al-Attar, D. (2016). Global dynamic topography observations reveal limited influence of large-scale mantle flow. *Nature Geoscience*, *9*, 456–463. https://doi.org/10.1038/ngeo2709

Holbrook, W. S., Mooney, W. D., & Christensen, N. I. (1992). The seismic velocity structure of the deep continental crust. In D. Fountain, R. Arculus, & R. Kay (Eds.), *Continental lower crust* (Vol. 23, pp. 1–43). New York: Elsevier.

Husson, L., Bernet, M., Guillot, S., Huyghe, P., Mugnier, J. L., Replumaz, A., … Van der Beek, P. (2014). Dynamic ups and downs of the Himalaya. *Geology*, *42*, 839–842. https://doi.org/10.1130/G36049.1

Keppie, J., Dostal, J., & Murphy, J. (2011). Complex geometry of the Cenozoic magma plumbing system in the central Sahara. NW Africa, ISI. ISSN: 0020-6814 (Print) 1938-2839 (Online) J. homepage: http://www.tandfonline.com/loi/tigr20

Klitzsch, E. (1971). The structural development of parts of North Africa since Cambrian time. In C. Gray (Ed.), *Symp. on the geology of Libya: Tripoli* (pp. 256–260). University of Libya: Faculty of Sciences.

Langston, C. A. (1979). Structure under Mount Rainier, Washington, inferred from teleseismic body waves. *Journal of Geophysical Research*, *84*, 4749–4762. https://doi.org/10.1029/JB084iB09p04749

Lemnifi, A. A., Liu, K. H., Gao, S. S., Reed, C. A., Elsheikh, A. A., Yu, Y., & Elmelade, A. A. (2015). Azimuthal anisotropy beneath north central Africa from shear wave splitting analyses. *Geochemistry, Geophysics, Geosystems*, *16*, 1105–1114. https://doi.org/10.1002/2014GC005706

Lemnifi, A. A., Elshaafi, A., Karaoğlu, Ö., Salah, M. K., Aouad, N., Reed, C. A., & Yu, Y. (2017). Complex seismic anisotropy and mantle dynamic beneath Turkey. *Journal of Geodynamics*, 0264–3707. https://doi.org/10.1016/j.jog.2017.10.004

Lesquer, A., Takheris, D., Dautria, J., & Hadiouche, O. (1990). Geophysical and petrological evidence for the presence of anomalous upper mantle beneath Sahara basin (Algeria). *Earth and Planetary Science Letters*, *96*, 407–418. https://doi.org/10.1016/0012-821X(90)90016-Q

Liégeois, J. P., Abdelsalam, M. G., Ennih, N., & Ouabadi, A. (2013). Metacraton: Nature, genesis and behavior. *Gondwana Research*, *23*, 220–237. https://doi.org/10.1016/j.gr.2012.02.016.

Liégeois, J. P., Benhallou, A., Azzouni-Sekkal, A., Yahiaoui, R., & Bonin, B. (2005). The Hoggar swell and volcanism: Reactivation of the Precambrian Tuareg shield during Alpine convergence and West African Cenozoic volcanism. *Geological Society of America, Special Papers*, *388*, 379–400. https://doi.org/10.1130/0-8137-2388-4.379

Lithgow-Bertelloni, C., & Silver, P. G. (1998). Dynamic topography, plate driving forces and the African superswell. *Nature*, *395*, 269–272. https://doi.org/10.1038/26212

Liu, K. H., & Gao, S. S. (2010). Spatial variations of crustal characteristics beneath the Hoggar swell, Algeria, revealed by systematic analyses of receiver functions from a single seismic station. *Geochemistry, Geophysics, Geosystems*, *11*, Q08011. https://doi.org/10.1029/2010GC003091

Liu, L., & Gurnis, M. (2010). Dynamic subsidence and uplift of the Colorado Plateau. *Geology*, *38*, 663–666. https://doi.org/10.1130/G30624.1

Liu, L., Gao, S. S., Liu, K. H., & Mickus, K. (2017). Receiver function and gravity constraints on crustal structure and vertical movements of the Upper Mississippi Embayment and Ozark Uplift. *Journal of Geophysical Research: Solid Earth*, *122*, 4572–4583. https://doi.org/10.1002/2017JB014201

Lloyd, S., Van Der Lee, S., Frana, G. S., Assumcáo, M., & Feng, M. (2010). Moho map of South America from receiver functions and surface waves. *Journal of Geophysical Research*, *115*, B11315. https://doi.org/10.1029/2009JB006829

Makris, J., & Stobbe, C. (1984). Physical properties and state of the crust and upper mantle of the Eastern Mediterranean Sea deduced from geophysical data. *Marine Geology*, *55*, 347–363.
Makris, J., & Vees, R. (1977). Crustal structure of the Aegean Sea and the Islands Evia, Crete, Greece, obtained by refraction seismic experiments. *Journal of Geophysical Research*, *42*, 329–341.
Makris, J., & Yegorova, T. (2006). A 3-D density-velocity model between the Cretan Sea and Libya. *Tectonophysics*, *417*, 201–220. https://doi.org/10.1016/j.tecto.2005.11.003
Marone, F., Van Der Meijde, M., Van Der Lee, S., & Giardini, D. (2003). Joint inversion of local, regional and teleseismic data for crustal thickness in the Eurasia-Africa plate boundary region. *Geophysical Journal International*, *154*, 499–514. https://doi.org/10.1046/j.1365-246X.2003.01973.x
Moucha, R., & Forte, A. M. (2011). Changes in African topography driven by mantle convection. *Nature Geoscience*, *4*, 660–661. https://doi.org/10.1038/ngeo1235
Moucha, R., Forte, A. M., Rowley, D. B., Mitrovica, J. X., Simmons, N. A., & Grand, S. P. (2009). Deep mantle forces and the uplift of the Colorado Plateau. *Geophysical Research Letters*, *36*, L19310. https://doi.org/10.1029/2009GL039778
Nair, S. K., Gao, S. S., Liu, K. H., & Silver, P. G. (2006). Southern African crustal evolution and composition: Constraints from receiver function studies. *Journal of Geophysical Research*, *111*, B02304. https://doi.org/10.1029/2005JB003802
Nixon, S., Maclennan, J., & White, N. (2011). *Generation of alkali and tholeiitic basalts: The Al Haruj volcanic field*, Paper presented at Volcanic and Magmatic Studies Group Annual Meeting, Queen's College Cambridge.
Nyblade, A., Suleiman, I., Roy, R., Pusell, B. A., Suleiman, A., Doser, D., & Keller, R. (1996). Terrestrial heat flow in the Sirt Basin, Libya, and the pattern of heat flow across northern Africa. *Journal of Geophysical Research*, *101*, 17,737–17,746.
Oliveira, R. G., & Medeiros, W. E. (2012). Evidences of buried loads in the base of the crust of the Borborema Province (NE Brazil) from Bouguer admittance estimates. *Journal of South American Earth Sciences*, *37*, 60–76. https://doi.org/10.1016/j.jsames.2012.02.004
Owens, T. J., Zandt, G., & Taylor, S. R. (1984). Seismic evidence for an ancient rift beneath the Cumberland Plateau, Tennessee: A detailed analysis of broadband teleseismic *P* waveforms. *Journal of Geophysical Research*, *89*, 7783–7795. https://doi.org/10.1029/JB089iB09p07783
Pasyanos, M. E., & Nyblade, A. A. (2007). A top to bottom lithospheric study of Africa and Arabia. *Tectonophysics*, *444*, 27–44. https://doi.org/10.1016/j.tecto.2007.07.008.
Pasyanos, M. E., & Walter, W. R. (2002). Crust and upper-mantle structure of North Africa, Europe and the Middle East from inversion of surface waves. *Geophysical Journal International*, *149*, 463–481. https://doi.org/10.1046/j.1365-246X.2002.01663.x
Pirajno, F. (2004). Hotspots and mantle plumes: Global intraplate tectonics, magmatism and ore deposits. *Journal of Petroleum Science and Engineering*, *82*, 183–216. https://doi.org/10.1007/s00710-004-0046-4
Priestley, K., & McKenzie, D. (2006). The thermal structure of the lithosphere from shear wave velocities. *Earth and Planetary Science Letters*, *244*, 285–301. https://doi.org/10.1016/j.epsl.2006.01.008
Reed, C. A., Almadani, S., Gao, S. S., Elsheikh, A. A., Cherie, S., Abdelsalam, M. G., … Liu, K. H. (2014). Receiver function constraints on crustal seismic velocities and partial melting beneath the Red Sea rift and adjacent regions, Afar Depression. *Journal of Geophysical Research: Solid Earth*, *119*, 2138–2152. https://doi.org/10.1002/2013JB010719.
Rudnick, R. L., & Fountain, D. M. (1995). Nature and composition of the continental crust: A lower crustal perspective. *Reviews of Geophysics*, *33*, 267–309. https://doi.org/10.1029/95RG01302
Rudnick, R. L., & Gao, S. (2003). Composition of the continental crust. *The Crust*, *3*, 1–64. https://doi.org/10.1016/B0-08-043751-6/03016-4
Sandvol, E., Seber, D., Calvert, A., & Barazangi, M. (1998). Grid search modeling of receiver functions: Implications for crustal structure in the Middle East and North Africa. *Journal of Geophysical Research*, *103*, 26,899–26,917. https://doi.org/10.1029/98JB02238
Schmeling, H. (1985). Partial melt below Iceland: A combined interpretation of seismic and conductivity data. *Journal of Geophysical Research*, *90*, 10,105–10,116.
Siebert, L., & Simkin, T. (2002). Volcanoes of the world: An illustrated catalog of Holocene volcanoes and their eruptions, Global Volcanism Program Digital Inf. Ser., GVP-3, Washington, DC. http://www.volcano.si.edu/world/
Speranza, F., Minelli, L., Pignatelli, A., & Chiappini, M. (2012). The Ionian Sea: The oldest in situ ocean fragment of the world? *Journal of Geophysical Research*, *117*, B12101. https://doi.org/10.1029/2012JB009475
Stuart, F., Masoud, A., & Mark, D. (2014). The origin of Cenozoic magmatism of Libya. *Geophysical Research Abstracts* (Vol. 16, EGU2014-15877).
Suleiman, I. S. (1985). Gravity and heat flow studies in the Sirte Basin, Libya (PhD dissetation), University of Texas, El Paso.
Sumner, J. (1989). Regional geophysics of Arizona. In J. Jenny, & S. Reynolds (Eds.), *Geological evolution of Arizona* (Vol. 17, pp. 717–739). Tucson, AZ: Geological Society Digest.
Tontini, F. C., Graziano, F. L., Cocchi, C., Carmisciano, L., & Stefanelli, P. (2006). Determining the optimal Bouguer density for a gravity data set: Implications for the isostatic setting of the Mediterranean Sea. *Geophysical Journal International*, *169*, 380–388. https://doi.org/10.1111/j.1365-246X.2007.03340.x
Van Der Meijde, M., Juliá, J., & Assumpcáo, M. (2013). Gravity derived Moho for South America. *Tectonophysics*, *609*, 456–467. https://doi.org/10.1016/j.tecto.2013.03.023
Van Der Meijde, M., Van Der Lee, S., & Giardini, D. (2003). Crustal structure beneath broad-band seismic stations in the Mediterranean region. *Geophysical Journal International*, *152*, 729–739. https://doi.org/10.1046/j.1365-246X. 2003.01871.x
Vail, J. R. (1971). *Dikes swarms and volcanic activity in northeastern Africa*, Symposium Geology of Libya (pp. 341–347). University of Libya.
Watanabe, T. (1993). Effects of water and melt on seismic velocities and their application to characterization of seismic reflectors. *Geophysical Research Letters*, *20*, 2933–2936. https://doi.org/10.1029/93GL03170
Woollard, G. P. (1959). Crustal structure from gravity and seismic measurements. *Journal of Geophysical Research*, *64*, 1521–1544. https://doi.org/10.1029/JZ064i010p01521
Yu, Y., Song, J., Liu, K. H., & Gao, S. S. (2015). Determining crustal structure beneath seismic stations overlying a low-velocity sedimentary layer using receiver functions. *Journal of Geophysical Research: Solid Earth*, *120*, 3208–3218. https://doi.org/10.1002/2014JB011610
Zandt, G., & Ammon, C. J. (1995). Continental crust composition constrained by measurements of crustal Poisson's ratio. *Nature*, *374*, 152–154. https://doi.org/10.1038/374152a0
Zhu, L. P., & Kanamori, H. (2000). Moho depth variation in Southern California from teleseismic receiver functions. *Journal of Geophysical Research*, *105*, 2969–2980. https://doi.org/10.1029/1999JB900322